Research Article

Journal of Environmental Nanotechnology

Hydrothermal Synthesis and Enhanced Corrosion Inhibition Activity of CdS QDs toward Zn Surface

K. Kandasamy[1], P. Rajasingh[2*]

[1]Department of Chemistry, K.S.R College of Arts and Science for Women, Tiruchengode, TN, India
[2]Department of Chemistry, Chikkanna Government Arts College, Tiruppur, TN, India
Received: 10.04.2021 Accepted: 05.05.2021
*sprajasingh@gmail.com

ABSTRACT

The hydrothermal method was used to synthesize hexagonal 3-5 nm CdS QDs with Delonix elata leaves aqueous extract as a capping agent. The synthesized CdS QDs were characterized by FTIR, UV-Vis, XRD, FESEM spectroscopy. The anticorrosion activity of CdS QDs coated Zn plate was exanimated under 1 M HCl, 6 M KOH, 3.5% NaCl electrolytic medium. The best corrosion resistance was achieved through the application of the CdS QDs coating on the Zn metal surface.

Keywords: Delonix elata; Hexagonal CdS QDs; Hydrothermal method; Anticorrosion activity.

1. INTRODUCTION

Zinc-based alloys and zinc oxide are used in various applications in the automobile, construction, light industry, batteries, and other industries. High quantities of zinc are used to produce die-castings, which are important in the automobile, electrical, and hardware industries. Zinc oxide is extensively used in the production of paints, rubber, cosmetics, inks, pharmaceuticals, and electrical equipment (Raja *et al.* 2016). Originally, a fresh zinc surface corrodes fairly quickly until it is enclosed with protective corrosion product films. In tremendously polluted industrial atmospheres, corrosion rate may rise with continued exposure. The corrosion rate in marine atmospheres has been found to decrease as the time of exposure increases (Quintana *et al.* 1996).

Delonix elata leaves aqueous extract has a natural capacity to act as a promising capping, stabilizing, and reducing agent in the synthesis of quantum dots. Through green synthetic protocols, *Delonix elata* leaves aqueous extract is used as an eco-friendly solvent and excellent capping agent in the fabrication of stable QDs. The plant extract-mediated cadmium sulfide quantum dots (CdS QDs) can be biocompatible and nontoxic (Abiola *et al.* 2010). They are extremely promising organic corrosion inhibitors and can act as photosensitizers for treating cancer. The high toxicity of chemical corrosion inhibitors leads to the search for green corrosion inhibitors as they are biodegradable and do not contain heavy metals and toxic substances (Gerengi *et al.* 2012). Additionally, plant products are inexpensive, readily available, renewable, and nontoxic. Plants contain a lot of phytochemicals like tannins, flavonoids, alkaloids, organic amino acids, pigments and dyes (Rani *et al.* 2012).

There is only a little information available about the processes of corrosion of zinc exposed to environmental conditions. So herein, CdS QDs were designed as a corrosion inhibitor and synthesized using *Delonix elata* leaves aqueous extract via a one-pot hydrothermal protocol.

2. EXPERIMENTAL SECTION

2.1 Materials

Reagent grade cadmium chloride ($CdCl_2.H_2O$), sodium sulfide ($Na_2S.H_2O$), polyvinylidene fluoride (PVDF), N-methyl-2-pyrrolidone (NMP) purchased were of the highest purity available and used without any further purification.

2.2 Synthesis of DCH (*Delonix elata* CdS QDs by Hydrothermal method)

The *Delonix elata* leaves water extract and DCH was prepared by using the procedure given in the literature (Kandasamy *et al.* 2020a; Sudha *et al.* 2021).

2.3 Characterization

XRD pattern of CdS QDs samples was characterized by CuKα (λ=1·5406 Å) radiation generated at 40 KeV, 40 mA and scanned in the 2θ range from 10 to 80°. At room temperature, an FT-IR spectrum was recorded in the range of 4000 to 400 cm-1. A Cary 5000 UV-Vis spectrophotometer has been used to evaluate the UV-visible maximum absorption spectrum of CdS QDs. A field transmission electron microscope was used to examine the scanning electron images.

2.4 Electrochemical measurements

A pure zinc metal plate was used to study the corrosive inhibition behavior. The Zn metal plate was consequently polished with 1 mm silicon carbide grit papers

and cleaned with acetone. The synthesized DCH was mixed with PVDF and NMP at 80:15:5 wt ratios to prepare a slurry. The slurry was further coated over on the metal surface of the Zn plate using the doctor blade technique. The coated plate was dried in an oven at 353 K for 1 h and then used for corrosion studies.

3. RESULT AND DISCUSSION

3.1 XRD analysis

Fig. 1 (a) shows that almost all of the peaks in the prepared samples can be correctly indexed into the hexagonal CdS phase (JCPDS card No. 41-1049). The Wurtzite (hexagonal) phase is the most stable compared to the others and is also the very easiest to synthesis. The peaks at 2θ = 25.30°, 27.04°, 28.34°, 36.64°, 44.22°, 48.26°, 52.31° are corresponding to the (1 0 0), (0 0 2), (1 0 1), (1 0 2), (1 1 0) and (1 0 3), respectively (Kandasamy *et al.* 2020) .

3.2 FT-IR Spectroscopy

The FTIR spectrum of the DCH sample was showed in Figure 1 (b). From these FTIR bands, the bands at 1603 cm^{-1}, 1390 cm^{-1}, 1254 cm^{-1}, and 1071 cm^{-1} correspond to the –C=O stretching, –C=H bending, –C-O and –C-N stretching vibrations; and the absorption bands in the 834 cm^{-1} and 543 cm^{-1} regions should correspond to the –C-Cl and –C-Br halide functional groups. The peak at 620 cm^{-1} confirms the formation of CdS QDs (Sudha *et al.* 2021).

3.3 UV-Vis spectrometer

The optical absorption of DCH was investigated by the UV-Vis absorption spectrum. It can be observed from Figure 1 (c), that the DCH sample at λ = 463 nm, which corresponds to the photoabsorption edge of CdS nanocrystals. The bandgap energy value is 2.37 eV(Kandasamy *et al.* 2020b).

3.4 FESEM analysis

The morphologies of DCH were observed by FESEM. The image in Figure 1(d) demonstrates that the DCH involves spherical shape particles with an average diameter of 5-7 nm. The size of DCH detected in FESEM images are corresponds to the XRD results. The similarities in particle size and thus the formation of CdS QDs are confirmed by comparing XRD and FESEM results (Lei *et al.* 2018).

3.5 Tafel curve measurement of DCH

The Tafel plots of pure Zn and DCH corrosion inhibitor/ Zn plate in three different aqueous electrolytes demonstrated namely Figure 2 (a) 1M HCl (b) 3.5% NaCl, (c) 6 M KOH. The corrosion rate was observed on pure Zn plates and DCH corrosion inhibitor coated Zn plates for all the electrolytes with -1.4 V to – 0.4 V. The corrosion potential value of the DCH/ Zn plate is moved towards the anodic region compared to the pure Zn plate. The corrosion rate (mm/year) was measured from the Tafel curve for Zn plate is 1.4356 (mm/year) and DCH/ Zn plate is 0.3821 (mm/year) for 1M HCl aqueous electrolyte (Table 1). Similarly, for the corrosion rate (mm/year) of Zn plates are 2.0642, 1.3465 and DCH/ Zn plates are 1.6881, 0.3189 (mm/year) for 3.5% NaCl, 6 M KOH, respectively. The DCH has a lower corrosion rate than pure Zn suggests that the improved corrosion resistance reached is due to the coating of DCH corrosion inhibitor over Zn metal surface. The corrosion-preventive nature of the DCH sample has been demonstrated in this study (Selvam *et al.* 2016).

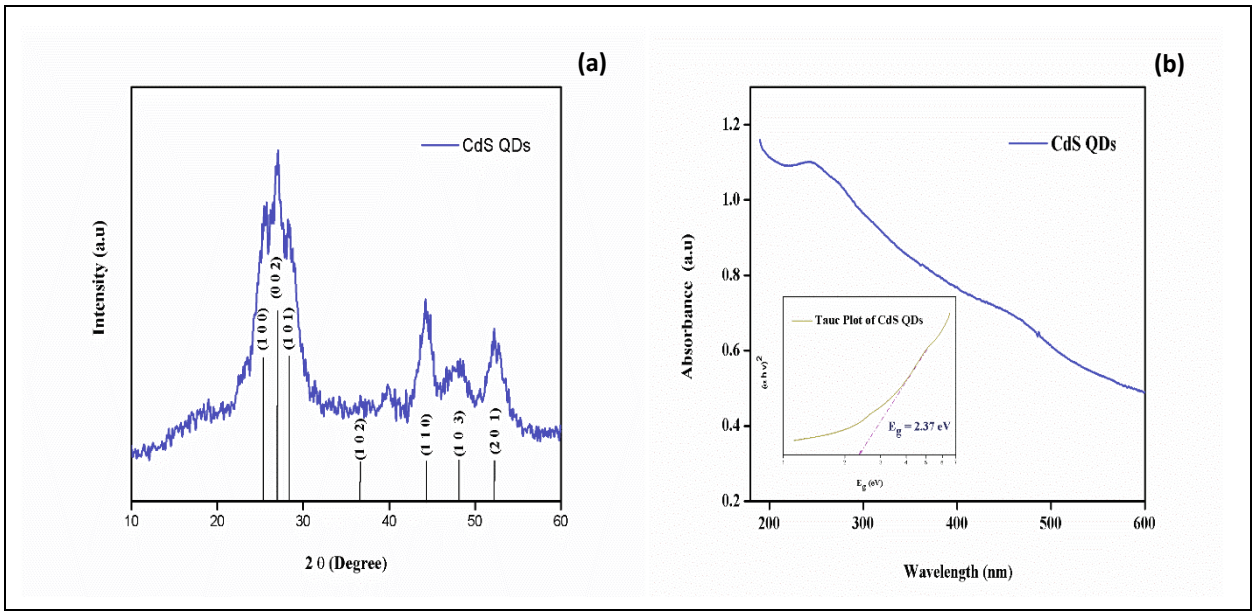

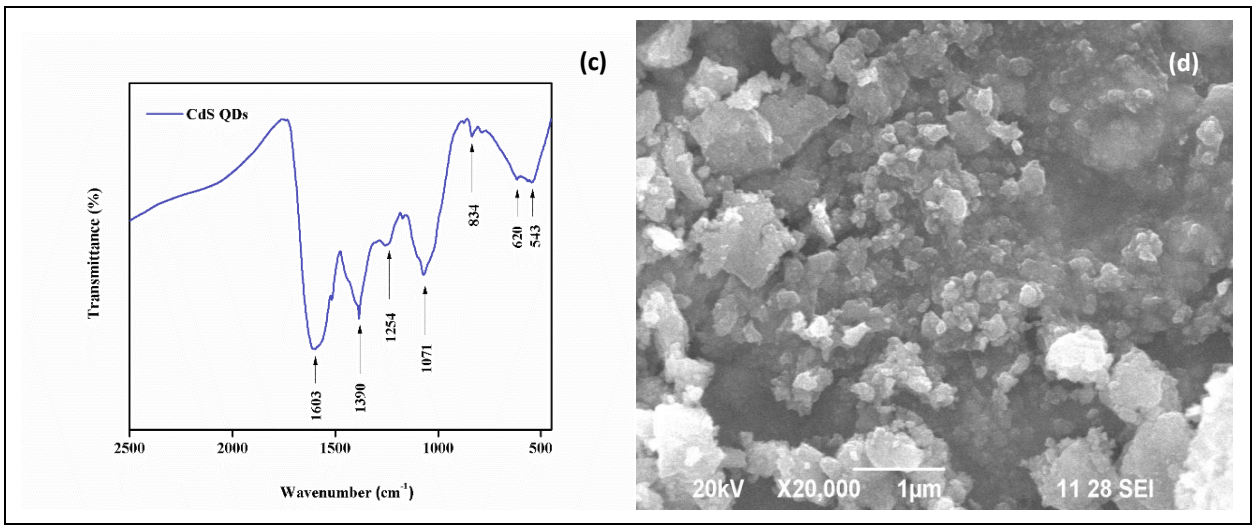

Fig. 1: (a) XRD, (b) FTIR (c) UV-Vis (d) FESEM Spectra for DCH sample

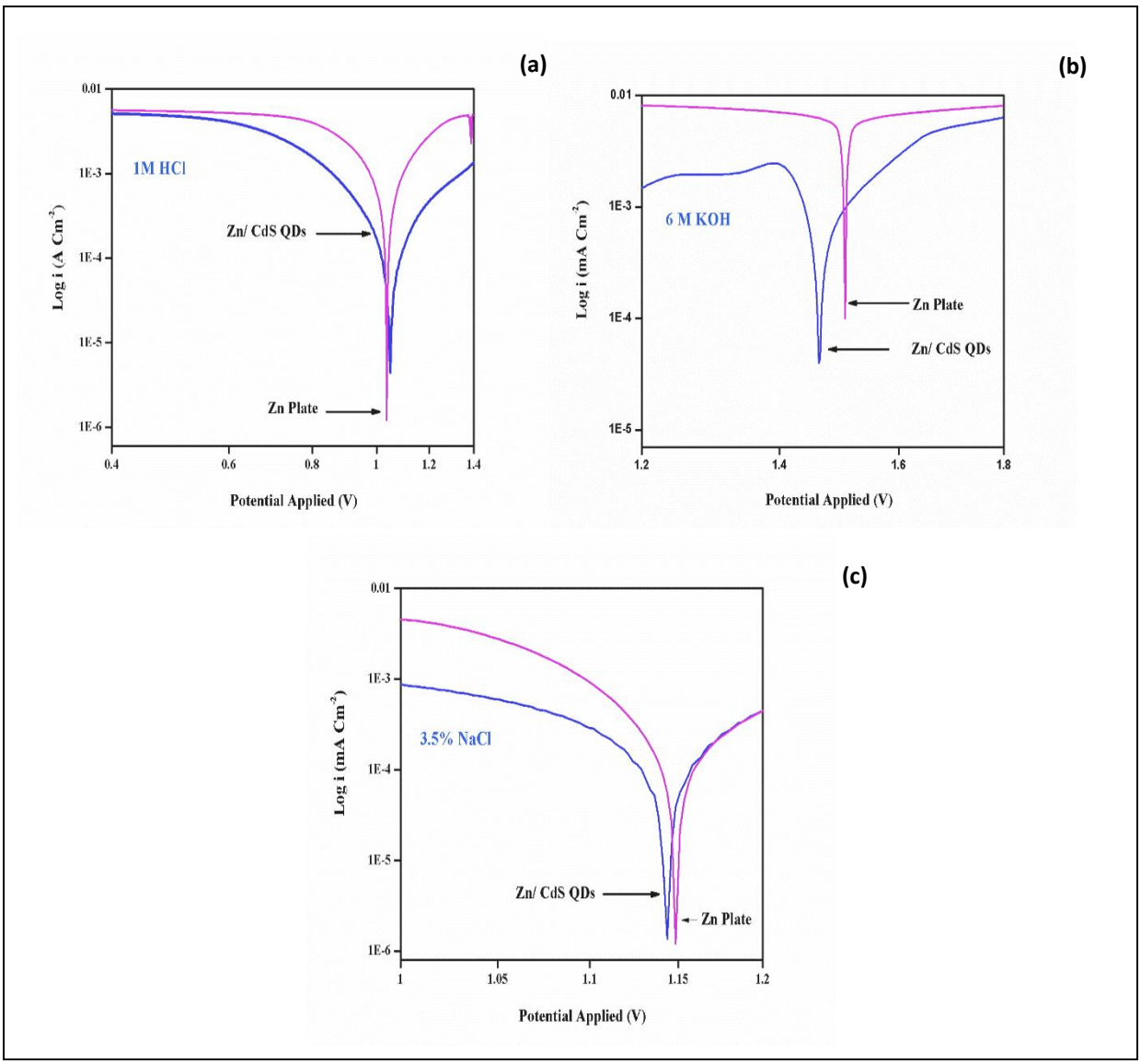

Fig. 2: (a) 1 M HCl, (b) 3.5 % NaCl (c) 6 M KOH Tafel curves for DCH sample

Table 1. The computed values of Tafel curves in 1 M HCl, 3.5 % NaCl, and 6 M KOH electrolytes

Electrolyte	Sample	Corrosion potential E_{corr} (mV)	Corrosion current I_{corr} (ACm^{-2})	Corrosion rate (mm/year)
1M HCl	Pure Zn	-1.1002	0.9697	1.4356
	DCH/ Zn plate	-1.0475	0.3288	0.3821
3% NaCl	Pure Zn	-1.2487	1.6998	2.0642
	DCH /Zn plate	-1.1433	1.5520	1.6881
6M KOH	Pure Zn	-1.6850	1.2554	1.3465
	DCH/ Zn plate	-1.4642	0.2745	0.3189

4. CONCLUSION

In conclusion, we have successfully developed a method to synthesize CdS QD using *Delonix elata* leave water extract by a hydrothermal method. The CdS QDs were tested in the corrosion inhibition activity of the Zn surface. The hexagonal (Wurtzite) phase and spherical shape of CdS QDs were confirmed by an XRD and FESEM, respectively. The as-synthesized material coated on zinc metal surface provided good corrosion protection. The hydrothermal method of synthesis may change the morphology of the product and thereby improve its corrosion activity.

5. REFERENCE

Abiola, O. K., James, A. O., The effects of Aloe vera extract on corrosion and kinetics of corrosion process of zinc in HCl solution, *Corros. Sci.* 52(2), 661–664 (2010). https://doi.org/10.1016/j.corsci.2009.10.026

Gerengi, H., Sahin, H. I., Schinopsis lorentzii Extract As a Green Corrosion Inhibitor for Low Carbon Steel in 1 M HCl Solution, *Ind. Eng. Chem. Res.* 51(2), 780–787 (2012). https://doi.org/10.1021/ie201776q

Kandasamy, K., Surendhiran, S., Syed Khadar, Y. A., Rajasingh, P., Ultrasound-assisted microwave synthesis of CdS/MWCNTs QDs: A material for photocatalytic and corrosion inhibition activity, Mater Today Proc. https://doi.org/10.1016/j.matpr.2020.07.080

Kandasamy, K., Venkatesh, M., Syed Khadar, Y. A., Rajasingh, P., One-pot green synthesis of CdS quantum dots using Opuntia ficus-indica fruit sap, *Mater. Today Proc.* 26, 3503–3506 (2020b). https://doi.org/10.1016/j.matpr.2019.06.003

Lei, R., Ni, H., Chen, R., Gu, H., Zhang, B., Zhan, W., Hydrothermal synthesis of CdS nanorods anchored on α-Fe2O3 nanotube arrays with enhanced visible-light-driven photocatalytic properties, *J. Colloid Interface Sci.* 514, 496–506 (2018). https://doi.org/10.1016/j.jcis.2017.12.061

Quintana, P., Veleva, L., Cauich, W., Pomes, R., Peña, J. L., Study of the composition and morphology of initial stages of corrosion products formed on Zn plates exposed to the atmosphere of southeast Mexico, *Appl. Surf. Sci.* 99(4), 325–334 (1996). https://doi.org/10.1016/0169-4332(96)00597-1

Raja, P. B., Ismail, M., Ghoreishiamiri, S., Mirza, J., Ismail, M. C., Kakooei, S., Rahim, A. A., Reviews on Corrosion Inhibitors: A Short View, *Chem. Eng. Commun.* 203(9), 1145–1156 (2016). https://doi.org/10.1080/00986445.2016.1172485

Rani, B. E. A., Basu, B. B. J., Green Inhibitors for Corrosion Protection of Metals and Alloys: An Overview, *Int. J. Corros.* 2012, 1–15 (2012). https://doi.org/10.1155/2012/380217

Selvam, M., Saminathan, K., Siva, P., Saha, P., Rajendran, V., Corrosion behavior of Mg/graphene composite in aqueous electrolyte, *Mater. Chem. Phys.* 172, 129–136 (2016). https://doi.org/10.1016/j.matchemphys.2016.01.051

Sudha, M., Surendhiran, S., Gowthambabu, V., Balamurugan, A., Anandarasu, R., Syed Khadar, Y. A., Vasudevan, D., Enhancement of Corrosive-Resistant Behavior of Zn and Mg Metal Plates Using Biosynthesized Nickel Oxide Nanoparticles, *J. Bio-Tribo-Corrosion* 7(2), 60 (2021). https://doi.org/10.1007/s40735-021-00492-w